# Dalton Transactions

Accepted Manuscript

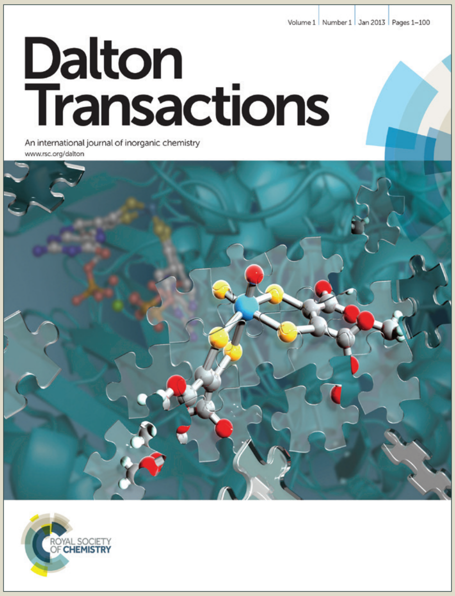

ROYAL SOCIETY OF CHEMISTRY

www.rsc.org/dalton

## Graphical abstract:

# Sulfonic acid-functionalized silica-coated magnetic nanoparticles as an efficient reusable catalyst for the synthesis of 1-substituted 1*H*-tetrazoles under solvent-free conditions

**Hossein Naeimi, Samaneh Mohamadabadi**

*Department of Organic Chemistry, Faculty of Chemistry, University of Kashan, Kashan, 87317, I.R. Iran. E-mail: naeimi@kashanu.ac.ir; Tel. No.: +98-361-5912388; Fax No.: +98-361-5912397*

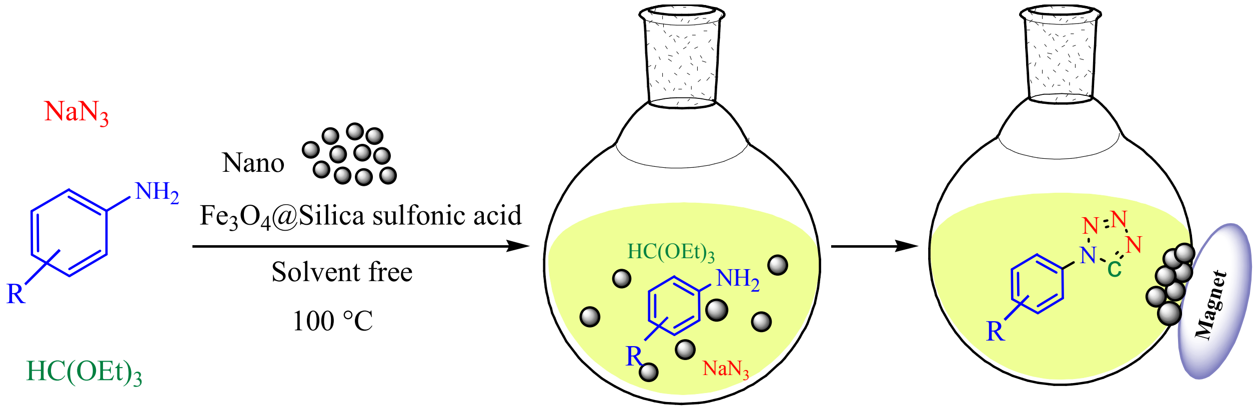

Dalton Transactions

RSCPublishing

ARTICLE

Cite this: DOI: 10.1039/x0xx00000x

Received 00th
Accepted 00th

DOI: 10.1039/x0xx00000x

www.rsc.org/

# Sulfonic acid-functionalized silica-coated magnetic nanoparticles as an efficient reusable catalyst for the synthesis of 1-substituted 1*H*-tetrazoles under solvent-free conditions

Hossein Naeimi*, Samaneh Mohamadabadi

*Department of Organic Chemistry, Faculty of Chemistry, University of Kashan, Kashan, 87317, I.R., Iran. E-mail: naeimi@kashanu.ac.ir; Tel: +98-361-5912388; Fax: +98-361-5912397.*

Regarding the green chemistry goals, silica-coated magnetite nanoparticles (MNPs) open up new avenue to introduce an amazing and efficient system for facilitating catalyst recovery in different organic reactions. Therefore, in this paper the preparation of sulfonic acid functionalized silica-coated magnetic nanoparticles with core-shell structure ($Fe_3O_4$@silica sulfonic acid) are presented by using $Fe_3O_4$ spheres as the core and silica sulfonic acid nanoparticles as the shell. The catalyst was characterized by infrared spectroscopy (FT-IR), scanning electron microscopy (SEM), X-ray diffraction analysis (XRD), dynamic light scattering (DLS), Thermo gravimetric analysis (TGA) and vibrating sample magnetometer (VSM). Nano catalyst can be recovered by an external magnet and reused for subsequent reactions for 6 times without noticeable deterioration in catalytic activity.

## Introduction

Magnetic iron oxide nanoparticles (NPs) have attracted much research interest over the recent years because of their unique physicochemical properties and great potential for various biomedical applications. In several pioneering works magnetic NPs were claimed as an effective tool for magnetically assisted biomolecule separation[1], biochemical sensing[2], NMR imaging[3,4], targeted drug delivery[5,6] and cancer treatment through hyperthermia[7,8]. The requirements for any biomedical application of magnetic nanoparticles include the chemical stability, biocompatibility, strong magnetization and low coercivity of the dispersed magnetic NPs.

Tetrazoles have a wide range of applications[9]. For example, this functional group has roles in material science including explosives and rocket propellants[10,11]. In addition, they can also function as ligands in coordination chemistry[12] and information recording systems[13].

Tetrazole can be prepared in several methods include acid-catalyzed cycloaddition between hydrazoic acid and isocyanides[14], acid-catalyzed cycloaddition between isocyanides and trimethyl azide[15], cyclization between primary amines, or their salts, with an orthocarboxylic acid ester in acetic acid or trifluoroacetic acid and sodium azide[16], and cyclizations from an amine, triethyl orthoformate, using AcOH, $PCl_5$, $In(OTf)_3$, $Yb(OTf)_3$, SSA, $[HBIm]BF_4$, natrolite zeolite, chitosan supported magnetic ionic liquid (CSMIL) and $Fe_3O_4@SiO_2$/Salen complex of Cu(II) as a catalyst[17-25].

In this work, the silica-coated magnetite nanoparticles are synthesized through two steps. The magnetite nanoparticles are firstly prepared by co-precipitation method. Then the magnetite nano particles are used to synthesize the $Fe_3O_4@SiO_2$ composite nanoparticles through the modified Stöber method[26]. Ability of this nano-magnetic solid acid catalyst in the one-pot three components reaction between triethyl orthoformate, an amine and sodium azide is also described. Utilization of easy reaction conditions, catalyst with high catalytic activity, good reusability, and simple magnetically work-up, makes this methodology as an interesting option for the economic synthesis of 1-substituted 1*H*-tetrazoles under solvent-free conditions.

## Results and discussion

### Preparation and characterization of the catalyst

$Fe_3O_4$@silica sulfonic acid core-shell composite, that $Fe_3O_4$ spheres as the core and silica sulfuric acid nanoparticles as the shell, was prepared by a simple, low cost and convenient method. Magnetite nanoparticles were synthesized by the co-precipitation route. To improve the chemical stability of magnetite nanoparticles, their surface engineering was successfully performed by the suitable deposition of silica onto nanoparticles surface by the ammonia-catalyzed hydrolysis of tetraethylorthosilicate (TEOS). Next, The $SiO_2$ spheres served as support for the immobilization of $SO_3H$ groups by simple mixing of core-shell composite and chlorosulfonic acid in $CH_2Cl_2$ (Scheme 1).

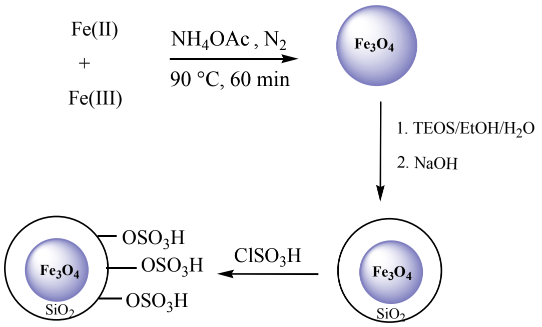

**Scheme 1** Preparation steps for fabricating sulfonic acid-functionalized magnetic $Fe_3O_4$ nanoparticles.

$Fe_3O_4$@silica sulfonic acid nanocomposite was characterized by FT-IR, XRD, TGA, SEM, DLS and VSM.
Figure 1 shows the FT-IR spectra of pure $Fe_3O_4$, $Fe_3O_4$@$SiO_2$ core/shell, and $Fe_3O_4$@silica sulfonic acid nanoparticles. The absorption peak at approximately 570 $cm^{-1}$ corresponding to the stretching vibration of the Fe–O bond and the adsorption of the silica-coated on the magnetite surface was indicated by band near 1100 $cm^{-1}$ assigned to the Si–O stretching vibration. Also, successful sulfonic acid functionalization of the silica layer on $Fe_3O_4$ surface was evidenced by the absorption bands at 1040 and 1130 $cm^{-1}$ are related to the stretching of the S–O bonds. A peak appeared at about 3400 $cm^{-1}$ due to the stretching of OH groups in the $SO_3H$ (Fig. 1c). These FT-IR spectra provided the formation of a silica shell onto the surface of $Fe_3O_4$ and the acid functionalization of the silica shell.

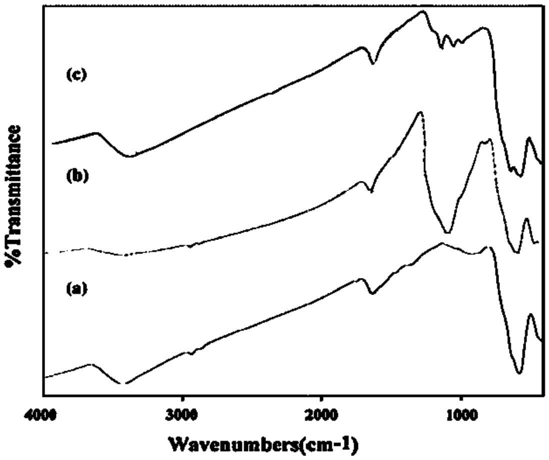

**Figure 1** comparative FT-IR spectra for (a) $Fe_3O_4$ (b) $Fe_3O_4$@$SiO_2$ (c) $Fe_3O_4$@silica sulfonic acid.

Figure 2 shows the X-ray diffraction patterns of magnetic nanoparticles. The observed diffraction peaks appeared at 2θ = 30.3°, 35.6°, 43.3°, 53.8°, 57.4° and 62.9° corresponding to the diffractions of (220), (311), (400), (422), (511) and (440) are indexed to the crystalline cubic inverse spinel structure of $Fe_3O_4$ nanoparticles. The sizes of the nanoparticles were evaluated from the XRD data using the Debye-Scherrer equation, which gives a relationship between particle size and peak broadening by the following equation:

$$d = k\lambda / (\beta \cos\theta)$$

where $d$ is the particle size of the crystal, $k$ is Sherrer constant (0.94), $\lambda$ is the X-ray wavelength (0.15406 nm), $\beta$ is the line broadening in radian obtained from the full width at half maximum (FWHM), and $\theta$ is the Bragg diffraction angle of the XRD diffraction patterns. The average MNPs core diameter was calculated to be 21 nm from the XRD results by above equation.

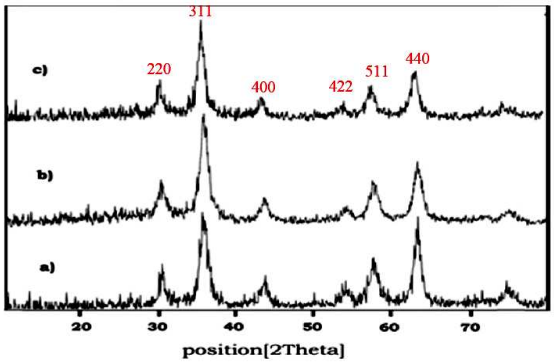

**Figure 2** XRD patterns of (a) $Fe_3O_4$ (b) $Fe_3O_4$@$SiO_2$ (c) $Fe_3O_4$@silica sulfonic acid.

TGA was used to study the thermal stability of the acid catalyst (Fig. 3). It is clear that, for the $Fe_3O_4$@silica sulfonic acid MNPs, there are three steps of weight loss in the following temperature ranges, namely; (1) below 150 °C, displayed a mass loss that was attributable to the loss of adsorbed solvent or trapped water from the catalyst. (2) Around 150-500 °C, the large weight reduction occurred in this region, which can be mainly resulted from the decomposition of $SO_3H$ groups (Fig. 3b). (3) Above 500 °C, the occurrence of further mass losses at higher temperature was resulted from the decomposition of silica shell[27].

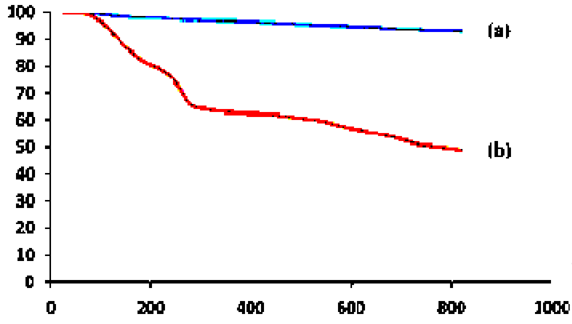

**Figure 3** TGA curve of (a) $Fe_3O_4$@$SiO_2$ (b) $Fe_3O_4$@silica sulfonic acid

The morphology and structure of prepared samples were characterized by scanning electron microscopy (SEM). Fig. 4a shows that the $Fe_3O_4$ nanoparticles are spherical in shape with an average size of 20 ± 2 nm, (b) shows that most of $Fe_3O_4$@$SiO_2$ nanoparticles are spherical with larger particle size and smoother surface. The SEM image shown in Fig. 4c demonstrates that $Fe_3O_4$@silica sulfonic acid nanoparticles are approximately spherical.

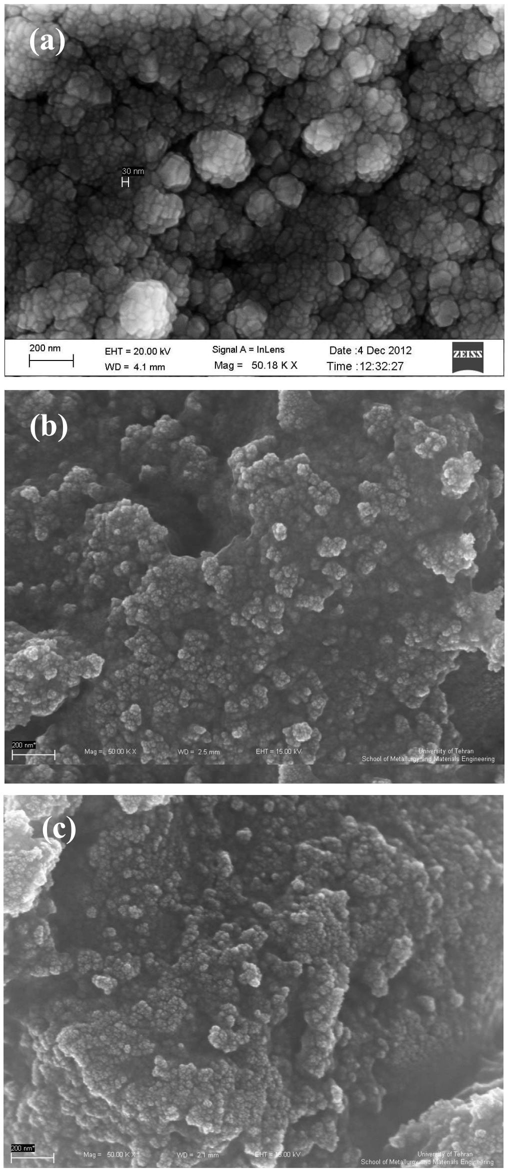

**Figure 4** SEM image of (a) $Fe_3O_4$ (b) $Fe_3O_4$@$SiO_2$ (c) $Fe_3O_4$@silica sulfonic acid

The dynamic light scattering (DLS) measurement of $Fe_3O_4$@silica sulfonic acid nanoparticles is shown in Fig. 5. In order to determine the fraction of the particle population that aggregates, comparisons between the intensity averaged DLS data and number averaged DLS data were made. From this slurry, an aqueous stock dispersion (100 ml acetone at 5 g $Fe_3O_4$@silica sulfonic acid) was prepared using an ultrasonic bath for 30 min.

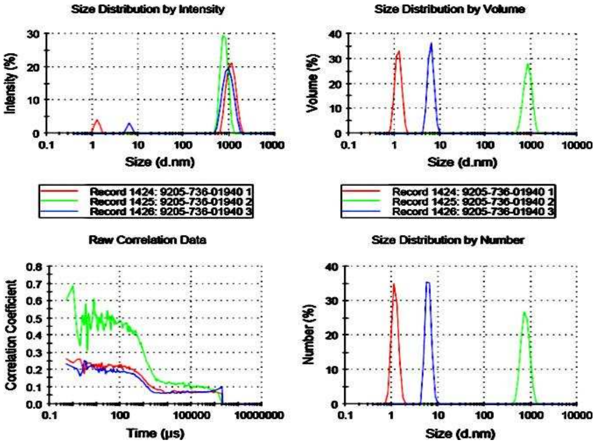

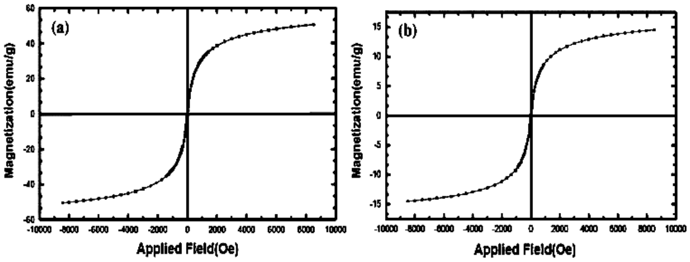

**Figure 5** DLS of $Fe_3O_4$@silica sulfonic acid

The magnetic property of the catalyst was studied by vibrating sample magnetometer (VSM). On the basis of Fig. 6, the saturation magnetization value was measured to be 50.86 emu/g for $Fe_3O_4$@$SiO_2$ and 14 emu/g for $Fe_3O_4$@silica sulfonic acid. The results are shown that the surface modification reaction has little impact on the magnetism of nano-adsorbent before and after modification and also the saturation magnetization of sulfonic acid-functionalized silica-coated magnetic nanoparticles is lower than that of $Fe_3O_4$@$SiO_2$ nanoparticles. Furthermore, the number of $H^+$ sites (0.33 mmol/g) for $Fe_3O_4$@silica sulfonic acid was quantitatively determined by acid-base titration [27].

**Figure 6** Magnetization curves for the prepared (a) $Fe_3O_4$@$SiO_2$ and (b) $Fe_3O_4$@silica sulfonic acid

### Optimization of the reaction conditions

For further studies regarding the effect of catalyst amount on formation of 1-substituted 1*H*-tetrazoles, we found that the yields were obviously affected by the amount of catalyst. It was found that 0.02 g $Fe_3O_4$@silica sulfonic acid was sufficient to catalyze the reaction of 4-chloro aniline, triethyl orthoformate and sodium azide at 100 °C (Table 1, entry 4). The usage of higher amounts of catalyst did not increase the yields significantly, while decreasing the amount of catalyst reduced the yields (Table 1). Also, when the reaction was attempted without the addition of catalyst, no desired product was obtained (Table 1, entry 1).

**Table 1** Effect of catalyst amount on formation of 1-Substituted 1*H*-tetrazoles.$^a$

| Entry | Cat. amount (g) | Time (min) | Yield$^b$ (%) |
|---|---|---|---|
| 1 | No catalyst | 300 | 0 |
| 2 | 0.005 | 150 | 65 |
| 3 | 0.01 | 120 | 82 |
| 4 | 0.02 | 80 | 95 |
| 5 | 0.03 | 50 | 80 |
| 6 | 0.05 | 50 | 63 |

[a] Reaction conditions: 4-chloro aniline (1 mmol), triethyl orthoformate (1.2 mmol), and sodium azide (1 mmol).
[b] Isolated yield.

After optimization of the reaction conditions, the reaction of triethyl orthoformate and sodium azide with various amines was carried out in according to the general experimental procedure (Scheme 2).

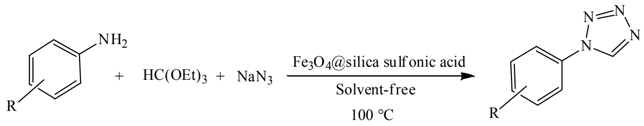

**Scheme 2** Synthesis of 1-substituted 1*H*-tetrazoles catalyzed by $Fe_3O_4$@silica sulfonic acid.

In all the cases, the corresponding 1-substituted 1*H*-tetrazoles were obtained in high to excellent yields and short reaction times. Therefore, we showed a reaction of several anilines with triethyl orthoformate, and sodium azide in the presence of 0.02 g $Fe_3O_4$@silica sulfonic acid, the results are summarized in Table 2.
A wide range of anilines containing electron-withdrawing groups and electron-donating groups such as, bromo, chloro, methyl and acetyl underwent condensation in short reaction times with excellent isolated yields. While, *para*-position anilines (Table 2, entries 3 and 4) were given good results in compared to the *ortho*-position anilines (Table 2, entries 6 and 10). There is more steric hindrance for the *ortho*- position anilines (*o*–Cl, –Me) on the product formation than the *para*- position (*p*–Cl, –Me) anilines. All known compounds were characterized by comparing their physical and spectral data with those reported in the literature.

**Table 2** Preparation of 1-substituted 1*H*-tetrazoles in the presence of $Fe_3O_4$@silica sulfonic acid$^a$.

| Entry | Substrate | product | Time (min) | Yield$^b$ (%) | TON |
|---|---|---|---|---|---|
| 1 | 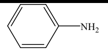<br>(1a) | 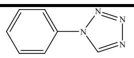<br>(3a) | 50 | 97 | 146.96 |
| 2 | 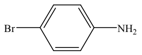<br>(1b) | 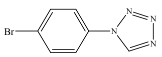<br>(3b) | 80 | 95 | 143.94 |
| 3 | 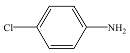<br>(1c) | 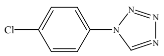<br>(3c) | 80 | 95 | 143.94 |
| 4 | 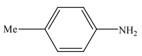<br>(1d) | 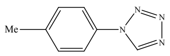<br>(3d) | 60 | 92 | 139.39 |
| 5 | 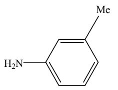<br>(1e) | 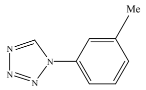<br>(3e) | 70 | 87 | 131.81 |
| 6 | 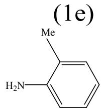<br>(1f) | 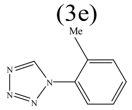<br>(3f) | 100 | 82 | 124.24 |
| 7 | 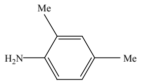<br>(1g) | 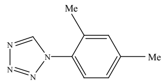<br>(3g) | 90 | 90 | 136.36 |
| 8 | 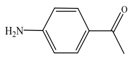<br>(1h) | 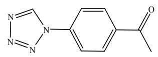<br>(3h) | 180 | 78 | 118.18 |
| 9 | 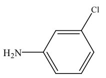<br>(1i) | 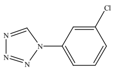<br>(3i) | 100 | 96 | 151.51 |
| 10 | 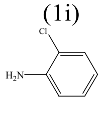<br>(1j) | 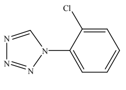<br>(3j) | 135 | 83 | 125.75 |
| 11 | 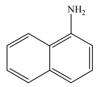<br>(1k) | 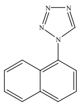<br>(3k) | 150 | 84 | 127.27 |

| | | | | | |
|---|---|---|---|---|---|
| 12 | 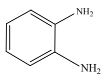<br>(1l) | 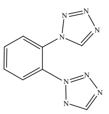<br>(3l) | 170 | 81 | 122.72 |

[a] Reaction conditions: amines (1 mmol), triethyl orthoformate (1.2 mmol), and sodium azide (1 mmol).
[b] Isolated yield.

### Reusability of the catalyst

The reusability is one of the important properties of this catalyst. The possibility and recovery of catalyst was investigated for the reaction of aniline, triethyl orthoformate, and sodium azide under optimized conditions. After completion of the model reaction, the catalyst was recovered from the reaction mixture simply by an external magnet. Then the recovered catalyst was washed with ethyl acetate, and reused for subsequent reactions for 6 times without noticeable deterioration in catalytic activity (Fig. 7).

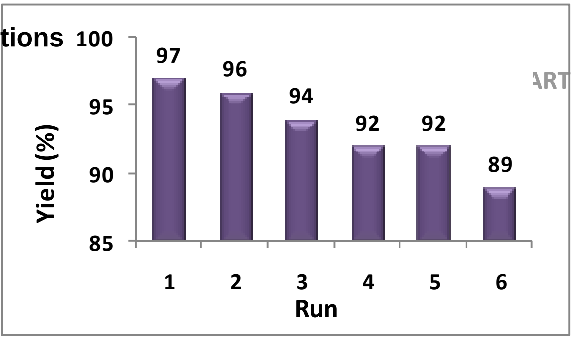

**Figure 7** Reusability of $Fe_3O_4$@silica sulfonic acid for the reaction of aniline, triethyl orthoformate, and sodium azide under solvent-free conditions

### Comparison of the $Fe_3O_4$@silica sulfonic acid catalyst with other catalysts

In future attempts, the activity of the prepared catalyst were measured in the model reaction. From Table 3, it was clear that $Fe_3O_4$@silica sulfonic acid remarkably worked well to give the desired product within 50 min in 97% yield in shorter reaction time and lower temperature than SSA and natrolite zeolite. Also this catalyst is comparable with $In(OTf)_3$, $[HBIm]BF_4$, CSMIL and $Fe_3O_4$@$SiO_2$/Salen Cu(II).

**Table 3** Comparison of different catalysts on formation of 1-substituted 1*H*-tetrazoles[a].

| Entry | Catalyst | solvent | t (°C) | Time (min) | Yield[b] (%) | Ref. |
|---|---|---|---|---|---|---|
| 1 | SSA | Neat | 120 | 300 | 95 | 20 |
| 2 | Natrolite zeolite | Neat | 120 | 240 | 82 | 22 |
| 3 | $In(OTf)_3$ | Neat | 100 | 90 | 89 | 18 |
| 4 | $[HBIm]BF_4$ | Neat | 100 | 30 | 91 | 21 |
| 5 | CSMIL | Neat | 70 | 60 | 92 | 23 |
| 6 | $Fe_3O_4$@$SiO_2$/Salen Cu(II) | Neat | 100 | 60 | 96 | 24 |
| 7 | $Fe_3O_4$@silica sulfonic acid | Neat | 100 | 50 | 97 | -- |

[a] Reaction conditions: aniline (1 mmol), triethyl orthoformate (1.2 mmol), and sodium azide (1 mmol), $Fe_3O_4$@silica sulfonic acid (0.02 g), solvent free at 100 °C.
[b] Isolated yield.

## Experimental section

### Chemicals

Iron (II) chloride tetrahydrate (99%), iron (III) chloride hexahydrate (98%), tetraethoxysilane (TEOS), chlorosulfonic acid and other chemical materials were purchased from Fluka and Merck companies and used without further purification.

### Apparatus

Products were characterized by comparison of their physical data, IR and $^1H$ NMR and $^{13}C$ NMR spectra with known samples. NMR spectra were recorded on a Bruker Advance DPX 400 MHz instrument spectrometer at 400 and 100 MHz in $CDCl_3$ as solvent in the presence of TMS as internal standard. IR spectra were recorded as KBr pellets on a Perkin-Elmer 781 spectrophotometer. The purity determination of the products and reaction monitoring were accomplished by TLC on silica gel PolyGram SILG/UV 254 nm plates. X-ray diffraction patterns of samples were taken on a Philips Xpert X-ray powder diffraction diffractometer (CuK, radiation, k =0.154056 nm). The particle morphology was examined by SEM (Hitachi S4160 scanning electron microscope). TGA patterns were obtained for characterization of the heterogeneous catalyst on a Rheometric Scientific Inc. 1998 thermal analysis apparatus under a $N_2$ atmosphere. DLS was performed on Malvern ZEN 3600. Melting points were measured on a Yanagimoto micro melting point apparatus. The Bandelin ultrasonic HD 3200 with probe model KE 76.6 mm diameter was used to produce ultrasonic irradiation.

### Preparation of $Fe_3O_4$ (MNPs)

Magnetic nanoparticles were synthesized by co-precipitation of $FeCl_3.6H_2O$ and $FeCl_2.4H_2O$ in ammonia solution, according to the reported procedure[27]. Typically, $FeCl_3.6H_2O$ (15.136 g) and $FeCl_2{\cdot}4H_2O$ (6.346 g) were dissolved in 0.64 L deionized water under nitrogen at 90 °C and added to a ammonium hydroxide 25% solution (0.08 L) with vigorous mechanical stirring. After the color of bulk solution turned to black the reaction was carried out for 60 min in $N_2$ atmosphere. The resulting black MNPs were isolated by applying an external magnet, washed 3 times with deionized water and then dried under vacuum at 60 °C for 12 h.

### Preparation of $Fe_3O_4$@$SiO_2$

The $Fe_3O_4$@$SiO_2$ nanospheres were prepared by a modified Stöber method. Briefly, $Fe_3O_4$ (0.50 g) was dispersed in the mixture of ethanol (50 mL), deionized water (5 mL) and tetraethoxysilane (TEOS) (0.20 mL), followed by the addition of 5.0 mL of NaOH (10 wt%). This solution was stirred mechanically for 30 min at room temperature. Then the product, $Fe_3O_4$@$SiO_2$, was separated by an external magnet and was washed with deionized water and ethanol three times and dried at 80 °C for 10 h.

### Preparation of $Fe_3O_4$@silica sulfonic acid

A suction flask was equipped with a constant pressure dropping funnel. The gas outlet was connected to a vacuum system through an adsorbing solution of alkali trap. $Fe_3O_4$@silica (0.5 g) was added into the flask and dispersed by ultrasonic irradiation for 10 min in dry $CH_2Cl_2$ (10 mL). Chlorosulfonic acid (0.4 mL) was added drop wise to a cooled ice-bath over a period of 30 min at room temperature. After completion of the addition, the mixture was shaken for 90 min, while the residual HCl was eliminated by suction. Then the $Fe_3O_4$@silica sulfonic acid was separated from the reaction mixture by a magnetic field and washed several times with dried $CH_2Cl_2$. Finally, $Fe_3O_4$@silica sulfonic acid was dried under vacuum at 60 °C.

### General synthesis for the preparation of 1-substituted 1*H*-tetrazoles

A mixture of amine (1 mmol), sodium azide (1 mmol), triethyl orthoformate (1.2 mmol) and $Fe_3O_4$@silica sulfonic acid (0.02 g) was taken in a round-bottomed flask and stirred at 100 °C. The progress of the reaction was monitored by thin layer chromatography (TLC). After completion of the reaction, the reaction mixture was cooled to room temperature and diluted with ethyl acetate (3×20 mL). The catalyst was removed by an external magnet, and then the resulting solution was washed with water and dried over anhydrous $Na_2SO_4$. After concentration, a crystallization step was performed using EtOAc-hexane (1:9). The products were characterized by $^1$H NMR, $^{13}$C NMR, FT-IR and melting points. We have reported the spectral data of synthesized compounds.

**1-(phenyl)-1*H*-tetrazole (3a).** Yellow solid (97% yield); m.p= 63-65 °C. M.P$_{Lit}$: 65-67 °C; IR (KBr)/ ν (cm$^{-1}$): 3126 (C-H, sp$^2$ stretch Ar), 1694 (C=N), 1597, 1498 (C=C). $^1$H NMR ($CDCl_3$, 400 MHz) δ (ppm): 7.07-7.34 (m, 5H, Ar), 8.20 (s, 1H tetrazole).

**1-(4-Bromophenyl)-1*H*-tetrazole (3b).** White solid (95% yield); m.p=169-170°C ; IR (KBr)/ ν (cm$^{-1}$): 3060 (C-H, sp$^2$ stretch, Ar), 1659 (C=N), 1576, 1482 (C=C); $^1$H NMR ($CDCl_3$, 400 MHz) δ (ppm): 6.92-6.94 (d, 2H), 7.40-7.42 (d, 2H), 8.09 (s, 1H tetrazole); $^{13}$C NMR ($CDCl_3$, 100 MHz) δ (ppm): 116.43, 120.76, 132.03, 143.99, 149.29.

**1-(4-Chlorophenyl)-1*H*-tetrazole (3c).** White solid (95% yield); m.p=153-155°C; M.PLit:155-156 °C; IR (KBr)/ ν (cm$^{-1}$): 3057 (C-H, sp$^2$ stretch, Ar), 1661 (C=N), 1485, 1581 (C=C) $^1$H NMR ($CDCl_3$, 400 MHz) δ (ppm): 6.98-7.00 (d, 2H), 7.27-7.29 (d, 2H), 8.09 (s,1H tetrazole); $^{13}$C NMR ($CDCl_3$, 100 MHz) δ (ppm): 120.35, 128.85, 129.47, 143.52, 149.50.

**1-(4-Methylphenyl)-1*H*-tetrazole (3d).** Light yellow solid (87% yield); m.p=92-99 °C; IR (KBr)/ ν (cm$^{-1}$): 3022 (C-H, sp$^2$ stretch, Ar), 2918(C-H, sp$^3$ stretch), 1664 (C=N), 1607, 1506 (C=C); $^1$H NMR ($CDCl_3$, 400 MHz) δ (ppm): 2.34 (s, 3H), 6.94-6.96 (d, 2H), 7.11-7.13 (d, 2H), 8.17 (s, 1H tetrazole); $^{13}$C NMR ($CDCl_3$, 100 MHz) δ (ppm): 20.79, 119.08, 129.63, 130.17, 142.95, 149.77.

**1-(3-Methylphenyl)-1*H*-tetrazole (3e).** White solid (85% yield); m.p=53-55 °C; IR (KBr)/ ν (cm$^{-1}$): 3167 (C-H, sp$^2$ stretch, Ar), 2923 (C-H, sp$^3$ stretch), 1690 (C=N), 1594, 1483 (C=C); $^1$H NMR ($CDCl_3$, 400 MHz) δ (ppm): 2.33 (s, 3H), 6.86 (s, 1H), 6.89- 6.91 (d, 2H), 7.18-7.22(t, 1H), 8.21 (s, 1H tetrazole); $^{13}$C NMR ($CDCl_3$, 100 MHz) δ (ppm): 21.43, 115.93, 119.97, 124.06, 129.19, 139.26, 145.28, 149.23.

**1-(2-Methylphenyl)-1*H*-tetrazole (3f).** White solid (82% yield); m.p=152-155 °C; IR (KBr)/ ν (cm$^{-1}$): 3015 (C-H, sp$^2$ stretch, Ar), 2870 (C-H, sp$^3$ stretch), 1664(C=N), 1488, 1590 (C=C); $^1$H NMR ($CDCl_3$, 400 MHz) δ (ppm): 2.33 (s, 3H), 7.02-7.03 (d, 1H), 7.05-7.07 (d, 1H), 7.18-7.22 (t, 2H), 8.08 (s, 1HTetrazole); $^{13}$C NMR ($CDCl_3$, 100 MHz) δ (ppm): 17.94, 117.68, 123.43, 127, 128.71, 130.72, 144.10, 147.78.

**1-(2,4-Dimethylphenyl)-1H-tetrazole (3g).** White solid (90% yield); m.p=133-135 °C; IR (KBr)/ ν (cm$^{-1}$): 3069 (C-H, sp$^2$ stretch, Ar), 2914 (C-H, sp$^3$ stretch), 1663 (C=N), 1495, 1607 (C=C); $^1$H NMR ($CDCl_3$, 400 MHz) δ (ppm): 2.29 (s, 3H), 2.30 (s, 3H), 6.94-6.96 (d, 1H), 6.98-7.00 (d, 1H), 7.02 (s, 1H), 8.00 (s, 1H tetrazole).

**1-(4-Acetylphenyl)-1*H*-tetrazole (3h).** Yellow solid (78% yield); m.p=175-176 °C; IR (KBr)/ ν (cm$^{-1}$): 3075 (C-H, sp$^2$ stretch, Ar), 2995 (C-H, sp3 stretch), 1669 (C=N), 1499, 1585 (C=C); $^1$H NMR ($CDCl_3$, 400 MHz) δ (ppm): 2.60 (S, 3H), 7.13-7.15 (d, 2H), 7.95-7.97 (d, 2H), 8.30 (s, 1H tetrazole).

**1-(3-Chlorophenyl)-1*H*-tetrazole (3i).** White solid (81% yield); m.p=137-139 °C; IR (KBr)/ ν (cm$^{-1}$): 3065 (C-H, sp$^2$ stretch, Ar), 1669 (C=N), 1473, 1586 (C=C). $^1$H NMR ($CDCl_3$, 400 MHz) δ (ppm): 6.92-6.94 (d, 1H) 7.07-7.09 (d, 2H) 7.26-7.27 (t, 1H), 8.14 (s, 1H tetrazole); $^{13}$C NMR (CDCl3, 100 MHz) δ (ppm): 117.45, 119.23, 123.73, 130.34, 135.12, 146.14, 149.72.

**1-(2-Chlorophenyl)-1*H*-tetrazole (3j).** White solid (79% yield); m.p=129-131 °C; IR (KBr)/ ν (cm$^{-1}$): 3023 (C-H, sp$^2$ stretch, Ar), 1670 (C=N), 1481, 1598 (C=C); $^1$H NMR ($CDCl_3$, 400 MHz) δ (ppm): 7.03-7.50 (m-4H), 8.10 (s, 1H tetrazole).

**1-(Naphthalen-1-yl)-1*H*-tetrazole (3k).** White solid (84% yield); m.p=132-135 °C; IR (KBr)/ ν (cm$^{-1}$): 3048 (C-H, sp$^2$ stretch, Ar), 1658(C=N), 1574, 1432 (C=C); $^1$H NMR ($CDCl_3$, 400 MHz) δ (ppm): 7.23-8.27 (m, 7H), 8.36 (s, 1H tetrazole).

**1-[2-(1*H*-tetrazol-1-yl) phenyl]-1*H*-tetrazole (3l).** White solid (83% yield); m.p=167-169 °C; IR (KBr)/ ν (cm$^{-1}$): 3062 (C-H, sp$^2$ stretch, Ar), 1619 (C=N) 1458, 1588 (C=C); $^1$H NMR ($CDCl_3$, 400 MHz) δ (ppm): 7.30-7.70 (m, 4H), 8.11 (s, 1HTetrazole); $^{13}$C NMR ($CDCl_3$, 100 MHz) δ (ppm): 115.76, 122.37, 138.50, 142.40.

## Conclusion

In conclusion, we have firstly reported that $Fe_3O_4$@silica sulfonic acid can be an efficient and reusable catalyst for one-pot synthesis of 1-substituted 1*H*-tetrazoles from an amine, triethyl orthoformate and sodium azide. The catalytic research on novel approaches toward magnetic nanoparticles should be improved to enhance organic synthesis. For that purpose, magnetic nanocatalyst provides high surface area for interaction of compounds. This catalyst can provide new way for continuous processes, because of its simple recyclability. Good yields, short reaction times, solvent-free conditions, non-toxic and a recyclable catalyst with a very easy operation are the most important advantages of synthesized catalyst. The catalyst can be easily recovered from the reaction system by an external magnet and reused for 6 times without noticeable deterioration in catalytic activity.

## Acknowledgement

The authors are grateful to University of Kashan for supporting this work by Grant No. 159148/43.

## Notes and References

1. O. Olsvik, T. Popovic, E. Skjerve, K. S. Cudjoe, E. Hornes, J. Ugelstad, M. Uhlen, *Clin. Microbiol. Rev*. 1994, **7**, 43–54.
2. M. N. Widjojoatmodjo, A. C Fluit, R. Torensma, J. Verhoef, *J. Immunol. Methods*. 1993, **165**, 11–19.
3. R. Weissleder, G. Elizondo, J. Wittenberg, C. A. Rabito, H. H. Bengele, L. Josephson, *Radiology*. 1990,**175**, 489–493.
4. J. W. M. Bulte, L. D. Ma, R. L. Magin, R. L. Kamman, C. E. Hulstaert, K. G. Go, T. H. The, L. de Leij, *Magn. Reson. Med*. 1993, **29**, 32–37.
5. P. K. Gupta, C. T. Hung, F. C. Lam, D. G. Perrier, *Int. J. Pharm*. 1988, **43**, 167–177.
6. T. Neuberger, B. Schöpf, H. Hofmann, M. Hofmann, B. von Rechenberg, *J. Magn. Magn. Mater*. 2005, **293**, 483–496.
7. A. Jordan, P. Wust, H. Fahling, R. Scholz, *Int. J. Hyperthermia*. 1993, **9**, 51–58.
8. U. Hafeli, W. Schutt, J. Teller, M. Zborowski, *Eds. Plenum Press*: New York and London, 1997, 527–534.
9. R.N. Butler, A.R. Katritzky, in *Comprehensive Heterocyclic Chemistry*, C.W. Rees, E.F.V. Scriven, Eds, Pergamon, Oxford, UK, 1996,Vol 4.
10. (a) V. A. Ostrovskii, M. S. Pevzner, T. P. Kofmna, M. B. Shcherbinin, I. V. Tselinskii, *Targets Heterocycl.Syst*. 1999, **3**, 467. (b) M. Hiskey, D. E. Chavez, D. L. Naud, S. F. Son, H. L. Berghout, C. A. Bome, *Proc. Int.Pyrotech. Semin*. 2000, *27*, 3.
11. M. U. S. Brown, Patent 3,338,915, 1967, *Chem. Abstr*. 1968, 87299.
12. (a) V.V. Nilulin, T.V. Artamonova, G.I. Koldobskii, Russ. *J. Org. Chem*. 2003, **39**, 1525-1529. (b) V.V. Nilulin, T.V. Artamonova, G.I. Koldobskii, Russ. *J. Org. Chem*. 2005, **41**, 444-445.
13. G.I. Koldobskii, V.A. Ostrovskii, *Usp. Khim*. 1994, **63**, 847.
14. (a) D. M. Zimmerman, R. A. Olofson, *Tetrahedron Lett*. 1969, **58**, 5081. (b) F. G. Fallon, R. M. Herbst, *J. Org. Chem*. 1957, **22**, 933.
15. T. Jin, S. Kamijo, Y. Yamamoto, *Tetrahedron Lett*. 2004, **45**, 9435.
16. Y. Satoh, N. Marcopulos, *Tetrahedron Lett*. 1995, **36**, 1759-1762.
17. A.K. Gupta, C.H. Oh, *Tetrahedron Lett*. 2004, **45**, 4113-4116.
18. K. Dhiman, M. Adinath, H. Alakananda, *Tetrahedron Lett*. 2009, **50**, 2668-2670.
19. W. Su, Z. Hong, W. Shan and X. Zhang, Eur. *J. Org. Chem*. 2006, 2723-2726.
20. D. Habibi, H. Nabavi, M. Nasrollahzadeh, *J. Chem*. 2012, 1-4.
21. T.M. Potewar, S.A. Siddiqui, R.J. Lahoti, K.V. Srinivasan, *Tetrahedron Lett*. 2007, **48**, 1721-1724.
22. D. Habibi, M. Nasrollahzadeh, T.A. Kamali, *Green Chem*. 2011, **13**, 3499-3504.
23. A. khalafi-Nezhad, S. mohammadi, *RSC Adv*. 2013, **3**, 4362-4371.
24. F. Dehghani, A.R. Sardarian, M. Esmaeilpour, *Journal of Organometallic Chemistry*. 2013, **743**, 87-96.
25. N. T. Pokhodylo, V. S. Matiychuk and M. D. Obushak, *Tetrahedron*, 2008, **64**, 1430.
26. W. Stöber, A. Fink, E. Bohn, *J. Colloid Interface Sci*. 1968, **26**, 62–69.
27. F. Nemati, M. M. Heravi, R. Saeedirad. *Chin. J. Catal*. 2012, **33**, 1825-1831.
28. K.D. Kim, S.S. Kim, Y.H. Choa, H.T. Kim, *J. Ind. Eng. Chem*. 2007, **13**, 1137–1141.